

## Influences of crystallization time and molar composition of hydrogel on the preparation of sodalite, cancrinite and analcime

X. Zhang\*, S. Jiang, S. Liu, L. Chen, L. Tong

*Key Laboratory of Micro-Nano Materials for Energy Storage and Conversion of Henan Province, Institute of Surface Micro and Nano Materials, College of Chemical and Materials Engineering, Xuchang University, Henan, 461000, China*

Sodalite, cancrinite and analcime were synthesized via hydrothermal processes, the influences of crystallization time and molar composition of hydrogel on the crystalline end products were investigated. The results revealed that with the prolongation of crystallization time from 3 min to 80 min, the crystallization followed a sequence of phase transformations from amorphous to zeolite NaA, sodalite and cancrinite. Well-crystallized cancrinite crystals were achieved at  $\text{Al}_2\text{O}_3/\text{SiO}_2$  molar ratios of 0.12, 0.34 and 0.76. However, with the  $\text{Al}_2\text{O}_3/\text{SiO}_2$  molar ratio was increased to 0.95, pure-form sodalite was formed. A gradual increase in the crystallinity of cancrinite was observed with increasing  $\text{H}_2\text{O}/\text{SiO}_2$  molar ratio, while too high  $\text{H}_2\text{O}/\text{SiO}_2$  resulted in analcime generated. Also, when the  $\text{Na}_2\text{O}/\text{SiO}_2$  molar ratios of the hydrogel were 0.70, 1.22 and 4.75, the corresponding products obtained were pure phases of analcime, cancrinite and sodalite, respectively.

(Received December 19, 2021; Accepted April 12, 2022)

*Keywords:* Crystallization, Synthesis, Crystal morphology, Sodalite, Cancrinite, Analcime

### 1. Introduction

Zeolites are crystalline aluminosilicates consisting of  $\text{SiO}_4^{4-}$  and  $\text{AlO}_4^{5-}$  tetrahedra [1,2]. The uniformly distributed cavities and channels in zeolites, usually the pore sizes range from 0.3–1 nm, endow them with unique molecular organization, recognition and discrimination properties [3,4]. Zeolites have been widely used as ion-exchangers, catalysts and adsorbents because of their high ion exchange capacity, strong acidity, superior thermal stability and good shape-selectivity [5–7].

Most of applications are closely related to zeolitic frameworks. Also, morphology and size of zeolite particles play important roles in the efficiency and mode of their applications. Nowadays, many attempts had been aimed at the studies of various factors which controlled the particulate shapes and crystallization pathways of zeolite samples. These results displayed that crystallization time and composition of hydrogel were very sensitive for zeolite formation [8–10]. Xu et al [11]. had synthesized sodalite membrane via a microwave-assisted hydrothermal method, the results

---

\* Corresponding author: zxx5973428@163.com

revealed that the initial product was both sodalite and zeolite NaA. While after 45 min, only pure-form sodalite membrane was formed. Similar results were observed by Peng and co-workers [12] who involved that the transformation by dissolution of zeolite NaA causing local supersaturation, nucleation of sodalite, and growth via Ostwald ripening. Also, Zhang et al. [13] synthesized zeolites NaA at room temperature, they found crystallization had been completed after 7 days, with the prolongation of reaction time, the particles transferred in shape, no other phase was observed. Kulprathipanja et al. [14] demonstrated that with batch molar ratio  $\text{SiO}_2/\text{Al}_2\text{O}_3 \leq 5$ , the synthesized products were low silica zeolites; while  $\text{SiO}_2/\text{Al}_2\text{O}_3 > 10$ , high silica zeolites such as beta, ZSM-5 and zeolites Y were formed. Additionally, Reyes et al. [15] pointed that the increase of  $\text{OH}^-$  concentration had reduced the polymerization of silicate species, high concentration of NaOH was in favor of LTA, JBW and analcime formation. From these literatures, the crystallinity would increase with prolonged crystallization time. However, zeolites were thermodynamically metastable stages, the formation of zeolite could not be on a thermodynamic basis alone because kinetics crystallization was also a crucial parameter to be considered.

In this work, attempt on the organic template-free hydrothermal synthesis of pure-form sodalite, cancrinite and analcime zeolite samples had been done. The influences of crystallization time and batch molar ratios  $\text{Al}_2\text{O}_3/\text{SiO}_2$ ,  $\text{H}_2\text{O}/\text{SiO}_2$  and  $\text{Na}_2\text{O}/\text{SiO}_2$  on the crystalline end products and particulate properties (crystal shape, crystal size) were studied.

## **2. Experimental**

### **2.1. Zeolite synthesis**

The products were prepared as followed: sodium hydroxide (99%, Merck) and sodium aluminate (anhydrous, Merck) were dissolved in distilled water. Afterwards a certain amount of colloidal silica suspension (ZS-30, Shangdong Yousuo Chemical Co. Ltd.) was slowly poured into the above solution under strong agitation, the resultant hydrogel with molar composition  $z \text{Na}_2\text{O} : x \text{Al}_2\text{O}_3 : 1.0 \text{SiO}_2 : y \text{H}_2\text{O}$ , where  $x$  varied from 0.01 to 0.95 mol,  $y$  from 14.2 to 62.8 mol and  $z$  from 0.23 to 4.75 mol, respectively. The hydrogel was agitated for 40 min, later stored in a convection oven ( $T = 190 \text{ }^\circ\text{C}$ ) in sealed Teflon-lined stainless steel autoclaves. Finally, the precipitates thus obtained were filtered and thoroughly washed with distilled water, then dried at  $90 \text{ }^\circ\text{C}$  overnight.

### **2.2. Characterization**

X-ray diffraction patterns (XRD) were taken by a PhilipsPW 1830 diffractometer with Cu-K $\alpha$  radiation operated at 20 mA and 40 kV. Scanning electron microscopy images (SEM) were performed by a LEO 1530 TFE microscope. Transmission IR spectra (FTIR) were made using a Bruker IFS 66 v/S spectrometer with samples pressed in KBr pellets.

## **3. Results and discussions**

### **3.1. Influence of crystallization time**

The XRD patterns of samples synthesized after various crystallization times from 1.33  $\text{Na}_2\text{O} : 0.17 \text{Al}_2\text{O}_3 : 1.0 \text{SiO}_2 : 27.8 \text{H}_2\text{O}$  are exhibited in Fig. 1. As seen in the figure, the product

obtained after 3 min crystallization is amorphous material (Fig. 1a). After 10 min, the product synthesized is a mixture of crystalline sodalite and zeolite NaA (Fig. 1b). While after 20 min, pure-form sodalite is achieved in the crystallized sample (Fig. 1c). Cancrinite accompany with a trace of sodalite are observed after 30 min crystallization (Fig. 1d). However, with the synthesis time is increased to 60 min, the sodalite peaks completely disappear and only pure phase cancrinite is observed (Fig. 1e). Further prolonging the crystallization time to 80 min, the relative intensity of diffraction peaks would not increase, indicating that the crystallization of cancrinite is almost complete within 60 min (Fig. 1f).

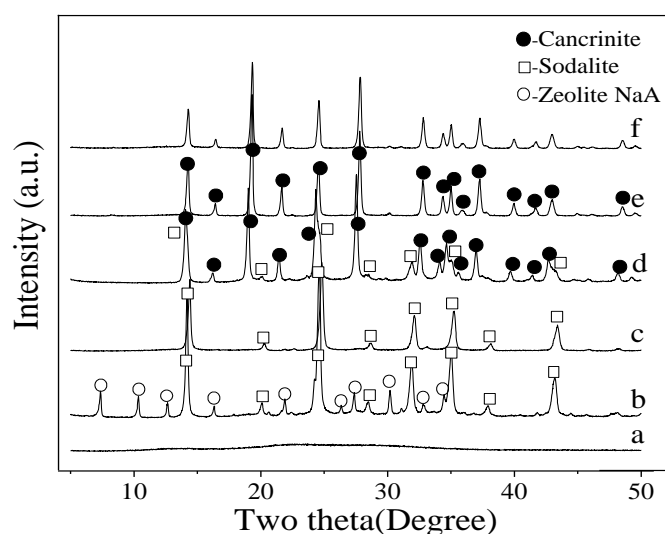


Fig. 1. X-ray diffraction patterns of products synthesized with various crystallization times. (a) 3 min, (b) 10 min, (c) 20 min, (d) 30 min, (e) 60 min, and (f) 80 min.

Fig. 2 displays pictures of products synthesized from various crystallization times. Clearly, the 3 min crystallized products consist of aggregated amorphous gel particles (Fig. 2a). Valtchev et al. [16] demonstrated the existence of nuclei wrapped by amorphous mass, which could be verified by synchrotron in situ XRD. After 10 min reaction, flower-like shaped morphology crystals due to sodalite and some spherical shaped zeolite NaA particles are formed (Fig. 2b). While after 20 min, the spherical shaped particles disappear and only flower-like particles of sodalite are observed (Fig. 2c). This may be explained that metastable zeolite NaA crystals were generated at the initial crystallization stage, which transformed into more thermodynamically stable sodalite phase with prolonged heating. With the reaction time is prolonged to 30 min, the product synthesized is a mixture of both sodalite and needle-type hexagonal crystals corresponding to cancrinite (Fig. 2d). Whilst, the sample generated after 60 min possesses only needle shaped crystals (Fig. 2e). These results are well matched with the XRD results. It was reported that the conversion of sodalite to cancrinite occurred by solution-mediated processes of dissolution of sodalite and precipitation of cancrinite, rather than via solid-state nucleation and growth of cancrinite [17]. Besides, the 80 min crystallized sample exhibits a similar morphology to that of 60 min crystallized sample, but with more regular shapes are observed, the dimensions of these needle shaped crystals are mainly from 50 to 120 nm in width and 200 to 800 nm in length (Fig. 2f). The above results confirm that the 60

min sample is fully crystalline in accordance with XRD studies, however, cancrinite particles would continue to grow, the nutrients are namely provided by dissolving less stable and smaller zeolite nanoparticles. Also, the system enters into the Ostwald ripening stage.

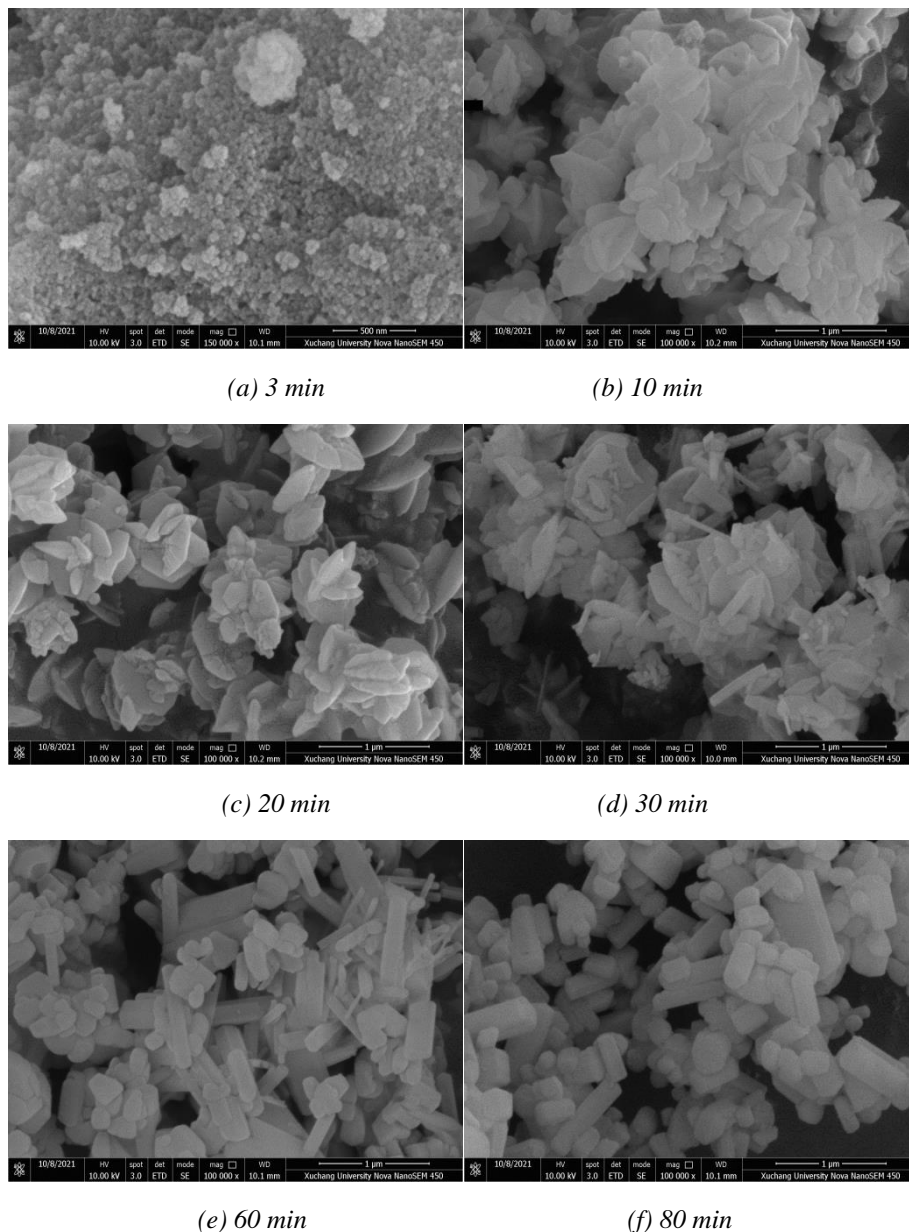


Fig. 2. SEM pictures of products synthesized with various crystallization times. (a) 3 min: amorphous material, (b) 10 min: NaA+sodalite, (c) 20 min: sodalite, (d) 30 min: sodalite+cancrinite, (e) 60 min: cancrinite, and (f) 80 min: cancrinite.

The corresponding FT-IR spectra of products are displayed in Fig. 3. The 3 min crystallized product without characteristic zeolite adsorption bands, implying it is amorphous material (Fig. 3a). After 10 min crystallization, the broad band at  $982\text{ cm}^{-1}$  correspond to the asymmetric stretching vibration of T-O-T (T= Al, Si); these sharp absorption bands at 725 and

$664\text{ cm}^{-1}$  are the characteristics of symmetric stretching of T–O–T; a band appears at  $465\text{ cm}^{-1}$  is ascribed to the bending vibration of O–T–O; while the band appears at  $429\text{ cm}^{-1}$  is due to the single four-membered ring (S4R) that is characteristic in the sodalite; the double four-membered ring (D4R) of zeolite NaA unit is confirmed at  $566\text{ cm}^{-1}$  (Fig. 3b) [18]. The band at  $566\text{ cm}^{-1}$  disappears with increasing crystallization time, indicating pure phase of sodalite sample is achieved (Fig. 3c). Additionally, after 30 min crystallization, new bands at  $626$  and  $577\text{ cm}^{-1}$  are detected which are characteristic of the cancrinite system (Fig. 3d) [19]. It was demonstrated that cancrinites and sodalites were naturally occurring minerals that belonged to the feldspathoid group, both of them were comprised of the ring with different stacking sequences [20]. While after 60 and 80 min crystallization, five absorption bands ( $469$ ,  $577$ ,  $626$ ,  $699$  and  $982\text{ cm}^{-1}$ ) are clearly observed (Fig. 3e–f). Similar results were reported by Borhade et al [21], who attributed these bands to the pure phase cancrinite units. These results are well matched with the XRD and SEM results.

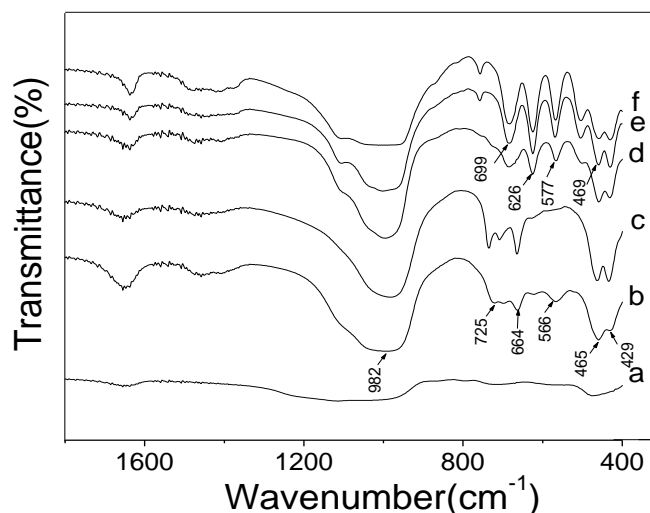


Fig. 3. IR spectra of products synthesized with various crystallization times. (a) 3 min, (b) 10 min, (c) 20 min, (d) 30 min, (e) 60 min, and (f) 80 min.

### 3.2. Influence of $\text{Al}_2\text{O}_3/\text{SiO}_2$ molar ratio

The XRD patterns of products synthesized in different  $\text{Al}_2\text{O}_3$  from  $1.33\text{ Na}_2\text{O} : x\text{ Al}_2\text{O}_3 : 1.0\text{ SiO}_2 : 27.8\text{ H}_2\text{O}$  after 80 min crystallization are displayed in Fig. 4. Clearly, the sample obtained at  $\text{Al}_2\text{O}_3/\text{SiO}_2=0.01$  is amorphous material (Fig. 4a). At  $\text{Al}_2\text{O}_3/\text{SiO}_2=0.04$ , the product synthesized is a mixture of both crystalline cancrinite and analcime (Fig. 4b). Well-crystallized pure phase cancrinite samples are achieved at relatively higher  $\text{Al}_2\text{O}_3/\text{SiO}_2$  molar ratios of 0.12, 0.34 and 0.76 (Fig. 4c–e). However, with the  $\text{Al}_2\text{O}_3/\text{SiO}_2$  molar ratio is increased to 0.95, a single phase sodalite is formed (Fig. 4f).

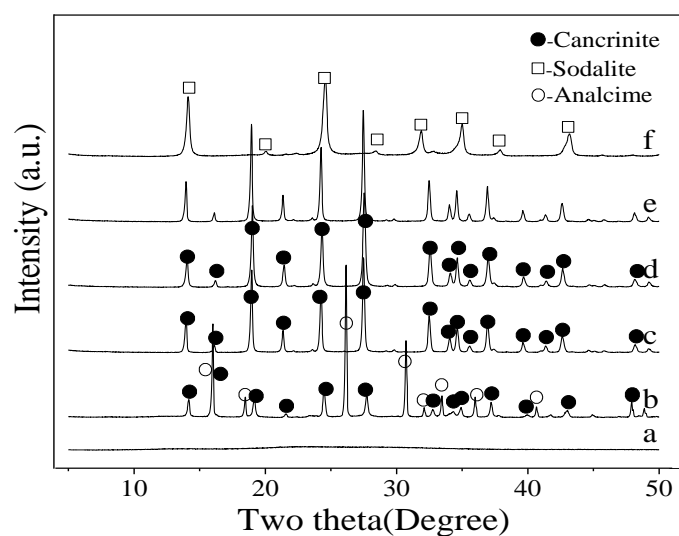


Fig. 4. X-ray diffraction patterns of products obtained from the hydrogel with various  $\text{Al}_2\text{O}_3/\text{SiO}_2$  molar ratios. x: (a) 0.01, (b) 0.04, (c) 0.12, (d) 0.34, (e) 0.76, and (f) 0.95.

The SEM pictures of products obtained with  $\text{Al}_2\text{O}_3/\text{SiO}_2$  molar ratios of 0.04, 0.12, 0.76 and 0.95 are exhibited in Fig. 5. As seen in the figure, polyhedral prismatic shaped morphology crystals due to analcime are seen in addition to the needle-like morphology of cancrinite with  $\text{Al}_2\text{O}_3/\text{SiO}_2=0.04$  (Fig. 5a). Generally, batch molar ratio  $\text{Al}_2\text{O}_3/\text{SiO}_2$  plays an important role in the zeolitic synthesis. The structure rearrangement happens and causes zeolite nuclei formation in the hydrogel, an appropriate atomic ratio Al/Si could contribute to the formation of a well-tuned precursor. Moreover, the  $\text{Al}_2\text{O}_3/\text{SiO}_2$  molar ratio increases with increasing sodium aluminate, the correspondingly higher  $\text{Al}^{3+}$  concentration favors small silicate species such as 6-membered rings formation. As a result, the products generated at  $\text{Al}_2\text{O}_3/\text{SiO}_2$  molar ratios of 0.12 and 0.76, only needle-like crystals corresponding to cancrinite are observed (Fig. 5b–c). Whilst, it is also observed that the sample synthesized with higher  $\text{Al}_2\text{O}_3/\text{SiO}_2$  favors the formation of cancrinite crystals with smaller particle diameter. The reason may be due to that higher  $\text{Al}_2\text{O}_3/\text{SiO}_2$  in the hydrogel would result in more pre-nuclei. Whereas at  $\text{Al}_2\text{O}_3/\text{SiO}_2=0.95$ , micro-sized spheres composed of submicron sodalite particles are obtained (Fig. 5d). The above results exhibit that, with the increasing  $\text{Al}_2\text{O}_3/\text{SiO}_2$  molar ratio in the hydrogel, the sequence of the end samples obtained is analcime, cancrinite and sodalite, respectively.

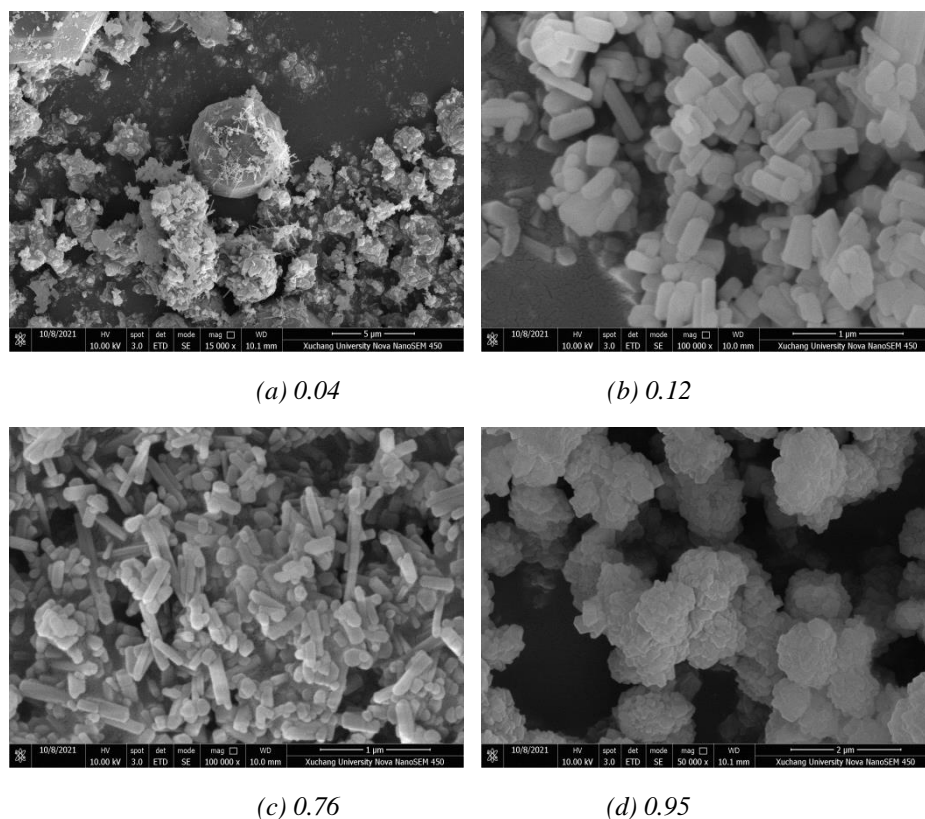


Fig. 5. SEM pictures of products synthesized from the hydrogel with various  $\text{Al}_2\text{O}_3/\text{SiO}_2$  molar ratios.  $x$ : (a) 0.04: analcime+cancrinite, (b) 0.12: cancrinite, (c) 0.76: cancrinite, and (d) 0.95: sodalite.

### 3.3. Influence of $\text{H}_2\text{O}/\text{SiO}_2$ molar ratio

The XRD patterns of products synthesized in different  $\text{H}_2\text{O}$  from  $1.33 \text{ Na}_2\text{O} : 0.17 \text{ Al}_2\text{O}_3 : 1.0 \text{ SiO}_2 : y \text{ H}_2\text{O}$  after 80 min crystallization are displayed in Fig. 6. Clearly, the product obtained at  $\text{H}_2\text{O}/\text{SiO}_2=14.2$  is ascribed to the relatively poorly crystallized cancrinite (Fig. 6a). Well-crystallized cancrinite samples are formed with the  $\text{H}_2\text{O}/\text{SiO}_2$  molar ratios of 18.7, 22.9 and 28.8, respectively (Fig. 6b–d). Ren et al [22]. had demonstrated that zeolites cannot be formed from a solvent-free route in the solid synthesis process, the introduction of a certain amount of water facilitated the reorganization processes, leading to enhanced crystalline phase formation [23]. However, too high  $\text{H}_2\text{O}/\text{SiO}_2$  molar ratio dilutes the concentrations of primary species in the system, resulting in lower nucleation and crystallization rates. For the product generated at  $\text{H}_2\text{O}/\text{SiO}_2=33.6$ , the lower intensity in XRD of cancrinite is observed (Fig. 6e). Whilst, further increasing the  $\text{H}_2\text{O}/\text{SiO}_2$  molar ratio to 41.2, the peaks of cancrinite weaken and those of analcime develop (Fig. 6f). It means that the composition of the mixture exceeds the area of single-phase sodalite existed in the  $\text{Na}_2\text{O}-\text{Al}_2\text{O}_3-\text{SiO}_2-\text{H}_2\text{O}$  quaternary system, the impurity phase of analcime is observed. Analcime is synthesized instead of cancrinite using more diluted activation solution, a single phase analcime is formed with  $\text{H}_2\text{O}/\text{SiO}_2=62.8$  (Fig. 6g).

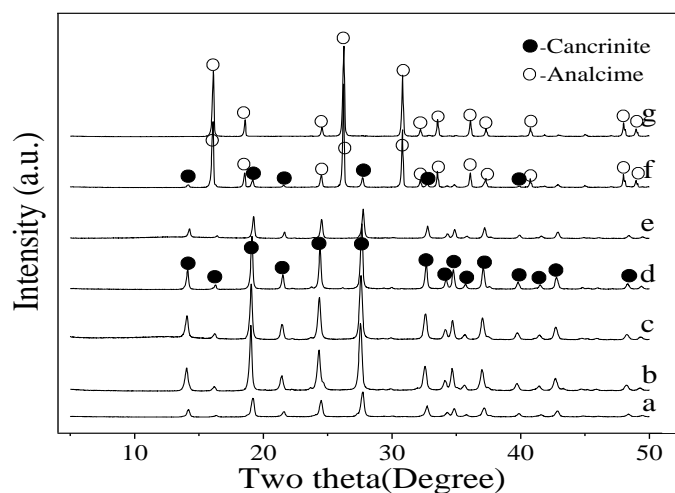


Fig. 6. X-ray diffraction patterns of products synthesized from the hydrogel with various  $H_2O/SiO_2$  molar ratios.  $y$ : (a) 14.2, (b) 18.7, (c) 22.9, (d) 28.8, (e) 33.6, (f) 41.2, and (g) 62.8.

### 3.4. Influence of $Na_2O/SiO_2$ molar ratio

The XRD patterns of products synthesized in different  $Na_2O$  from  $z Na_2O: 0.17 Al_2O_3: 1.0 SiO_2: 27.8 H_2O$  after 80 min crystallization are displayed in Fig. 7. Only amorphous materials are obtained at  $Na_2O/SiO_2=0.23$  (Fig. 7a). With  $Na_2O/SiO_2=0.48$ , analcime accompany with some unidentified phase are detected in the as-synthesized samples (Fig. 7b). Further increasing  $Na_2O/SiO_2$  molar ratio to 0.70, the XRD patterns for unidentified phase completely disappear and only pure analcime is observed (Fig. 7c). However, with  $Na_2O/SiO_2=1.0$ , the reaction leads to a mixture of analcime and cancrinite (Fig. 7d). When the  $Na_2O/SiO_2$  is increased to 1.22 and 2.34, pure-form cancrinite crystals with high crystallinity are obtained, respectively (Fig. 7e–f). The co-existence of cancrinite with sodalite at  $Na_2O/SiO_2=2.52$  (Fig. 7g). Whilst, in case of  $Na_2O/SiO_2=4.75$ , the peaks of cancrinite completely disappear and diffraction intensity of sodalite increases, implying pure-form sodalite is produced (Fig. 7h).

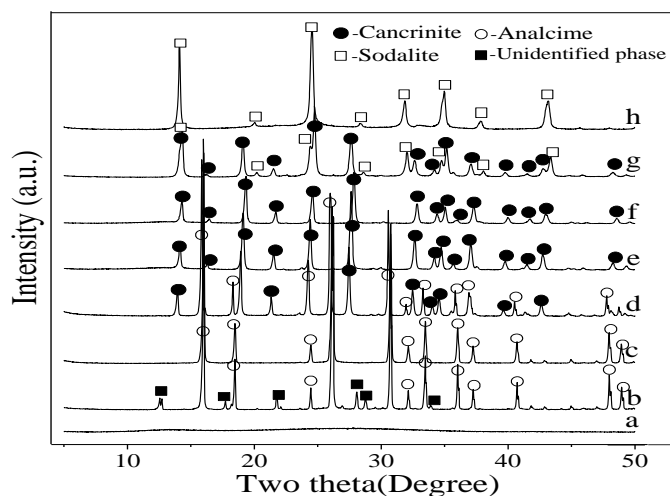


Fig. 7. X-ray diffraction patterns of products synthesized from the hydrogel with various  $Na_2O/SiO_2$  molar ratios.  $z$ : (a) 0.23, (b) 0.48, (c) 0.70, (d) 1.0, (e) 1.22, (f) 2.34, (g) 2.52, and (h) 4.75.

The SEM pictures of products obtained with  $\text{Na}_2\text{O}/\text{SiO}_2$  molar ratios of 0.23, 0.70, 1.0, 1.22, 2.34, and 4.75 are shown in Fig. 8. As can be seen, with  $\text{Na}_2\text{O}/\text{SiO}_2=0.23$ , a large number of amorphous materials are obtained (Fig. 8a). The product generated at  $\text{Na}_2\text{O}/\text{SiO}_2=0.70$  shows only good symmetry, polyhedral prismatic shaped morphology crystals corresponding to analcime, with a size ranging from 6 to 15  $\mu\text{m}$  (Fig. 8b). A large amount of needle shaped crystals adhered on the large analcime particles is seen with  $\text{Na}_2\text{O}/\text{SiO}_2=1.0$  (Fig. 8c). While only needle shaped particles of cancrinite are obtained with  $\text{Na}_2\text{O}/\text{SiO}_2$  molar ratios of 1.22 and 2.34 (Fig. 8d–e). From the above findings, it is seemed that lower alkalinity circumstance favors the analcime formation. Additionally, the cancrinite sample generated at  $\text{Na}_2\text{O}/\text{SiO}_2$  molar ratio of 1.22 shows the dimension of these particles is mainly from 80 to 150 nm in width and 110 to 600 nm in length. Whilst, the sample generated at  $\text{Na}_2\text{O}/\text{SiO}_2=2.34$  displays longer needle like shapes, with width vary from 40 to 60 nm, length vary from 200 to 800 nm are observed. An increase of alkalinity increased the concentration of structure forming  $\text{Na}^+$  ions which induced the formation of nuclei. Thus, the decrease of crystal size with increasing alkalinity can be readily explained by increased number of nuclei formed in the gel matrix. However, too strong alkalinity promotes the autolysis of samples obtained incipiently and leads to the decline in crystallinity, even impurity phase is generated. Fetchtelkord et al [24]. had demonstrated that sodalite was the thermodynamically more stable phase and the formation of cancrinite was kinetically favored at lower NaOH concentrations. This conclusion was not supported by Bian et al. [25], who argued that the transformation of sodalite to cancrinite occurred with the elevated NaOH concentrations. As shown in our case  $\text{Na}_2\text{O}/\text{SiO}_2=4.75$ , the micro-sized spheres composed of submicron particles identified as sodalite are formed (Fig. 8f).

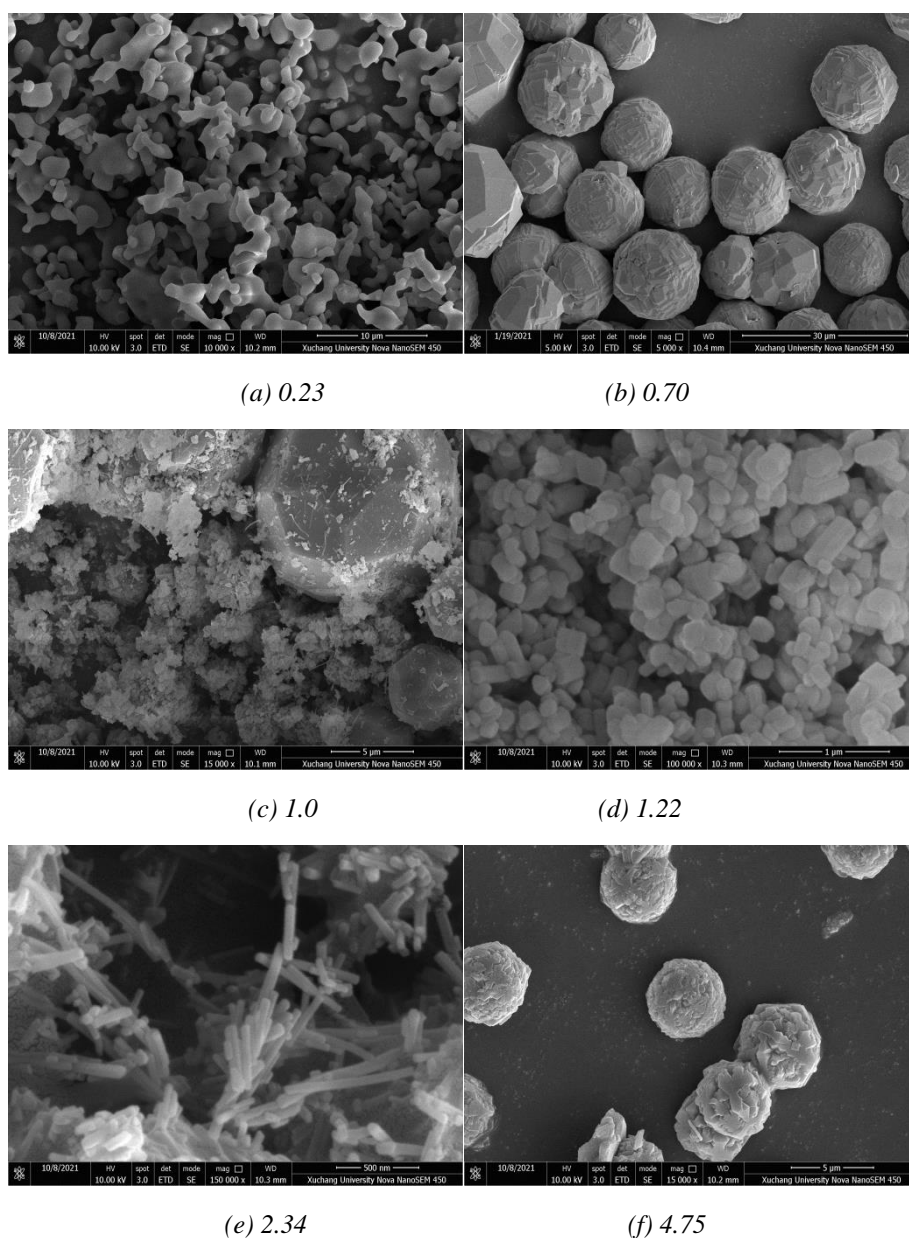


Fig. 8. SEM pictures of products synthesized from the hydrogel with various  $\text{Na}_2\text{O}/\text{SiO}_2$  molar ratios. z: (a) 0.23: amorphous material, (b) 0.70: analcime, (c) 1.0: analcime+ cancrinite, (d) 1.22: cancrinite, (e) 2.34: cancrinite, and (f) 4.75: sodalite.

#### 4. Conclusions

With the prolongation of crystallization time from 3 min to 80 min, the crystallization followed a sequence of phase transformations from amorphous to zeolite NaA, sodalite and cancrinite. Well-crystallized cancrinite samples were achieved at  $\text{Al}_2\text{O}_3/\text{SiO}_2$  molar ratios of 0.12, 0.34 and 0.76. However, with  $\text{Al}_2\text{O}_3/\text{SiO}_2=0.95$ , pure-form sodalite was formed. Also, the crystallinity of cancrinite gradually increased with increasing  $\text{H}_2\text{O}/\text{SiO}_2$  molar ratio, too high water content led to lower nucleation and crystallization rates; while  $\text{H}_2\text{O}/\text{SiO}_2=62.8$ , pure-form

analcime was generated. Additionally, the Na<sub>2</sub>O/SiO<sub>2</sub> molar ratio of the hydrogel was very sensitive for zeolitic synthesis. When the Na<sub>2</sub>O/SiO<sub>2</sub> molar ratios of the hydrogel were 0.70, 1.22 and 4.75, the corresponding samples obtained were analcime, cancrinite and sodalite, respectively.

### Acknowledgments

Financial supports by the College Natural Science Foundation of Henan Province (17B530004).

### References

- [1] R. M. Barrer, *Zeolites and Clay Minerals as Sorbents and Molecular Sieves*, Academic Press, London, 1978.
- [2] A. Dyer, *An Introduction to Zeolite Molecular Sieve*, John Wiley, London, 1988.
- [3] A. M. Manta, D. L. Cursaru, S. Mihai, *Dig. J. Nanomater. Bios.* 14, 509 (2019).
- [4] J. Wen, H. Dong, G. Zeng, *J. Clean. Prod.* 197, 1435 (2018)  
<https://doi.org/10.1016/j.jclepro.2018.06.270>
- [5] J. Zhao, L. Q. Yang, L. Yu, X. M. Zhao, Y. C. Hao, Z. J. Zhao, *Dig. J. Nanomater. Bios.* 16, 527 (2021).
- [6] P. Brea, J. A. Delgado, V. I. Águeda, P. Gutiérrez, M. A. Uguina, *Micropor. Mesopor. Mat.* 286, 187 (2019)  
<https://doi.org/10.1016/j.micromeso.2019.05.021>
- [7] M. Saifuddin, J. Bae, K. S. Kim, *Water Res.* 158, 246 (2019)  
<https://doi.org/10.1016/j.watres.2019.03.045>
- [8] X. Zhang, Q. Liu, S. Yang, *Dig. J. Nanomater. Bios.* 15, 769 (2020).
- [9] J. Zhu, Z. Liu, S. Sukenaga, M. Ando, H. Shibata, T. Okubo, T. Wakihara, *Micropor. Mesopor. Mat.* 268, 1 (2018). [https://doi.org/10.1016/S1387-1811\(01\)00279-7](https://doi.org/10.1016/S1387-1811(01)00279-7)
- [10] L. B. Bortolatto, R. A. A. Boca Santa, J. C. Moreira, D. B. Machado, M. A. P. M. Martins, M. A. Fiori, N. C. Kuhnen, H. G. Riella, *Micropor. Mesopor. Mat.* 248, 214 (2017)  
<https://doi.org/10.1016/j.micromeso.2017.04.030>
- [11] X. Xu, Y. Bao, C. Song, W. Yang, J. Liu, L. Lin, *Micropor. Mesopor. Mat.* 75, 173 (2004).  
<https://doi.org/10.1016/j.micromeso.2004.07.019>
- [12] H. Peng, D. Seneviratne, J. Vaughan, *Ind. Eng. Chem. Res.* 57, 1408 (2018)  
<https://doi.org/10.1021/acs.iecr.7b04538>
- [13] X. Zhang, D. Tong, W. Jia, D. Tang, X. Li, R. Yang, *Mater. Res. Bull.* 52, 96 (2014)  
<https://doi.org/10.1016/j.materresbull.2014.01.008>
- [14] S. Kulprathipanja, *Zeolites in industrial separation and catalysis*, Wiley-VCH Verlag GmbH & Co. KGaA, 2010. <https://doi.org/10.1002/9783527629565>
- [15] C. A. R. Reyes, C. D. Williams, O. M. C. Alarcon, *Rev. Fac. Ing. Univ. Antiquia N.* 53, 30 (2010).
- [16] V. P. Valtchev, K. N. Bozhilov, *J. Phys. Chem. B* 108, 15587 (2004).  
<https://doi.org/10.1021/jp048341c>

- [17] M. C. Barnes, J. Addai-Mensah, A. R. Gerson, *Micropor. Mesopor. Mat.* 31, 287 (1999).  
[https://doi.org/10.1016/S1387-1811\(99\)00079-7](https://doi.org/10.1016/S1387-1811(99)00079-7)
- [18] S. Alfaro, C. Rodríguez, M. A. Valenzuela, P. Bosch, *Mater. Lett.* 61, 4655 (2007).  
<https://doi.org/10.1016/j.matlet.2007.03.009>
- [19] P. Zhang, S. Li, C. Zhang, *Biomass Convers. Bior.* 9, 641 (2019)  
<https://doi.org/10.1007/s13399-019-00375-8>
- [20] F. Ocanto, R. Alvarez, B. Moy, M. Brikgi, C. U. Navarro, C. F. Linares, *J. Mater. Sci.* 43, 190 (2008). <https://doi.org/10.1007/s10853-007-2083-y>
- [21] A. V. Borhade, T. A. Kshirsagar, A. G. Dholi, J. A. Agashe, *J. Chem. Eng. Data*, 60, 586 (2015).
- [22] L. M. Ren, Q. M. Wu, C. G. Yang, L. F. Zhu, C. J. Li, P. L. Zhang, H. Y. Zhang, X. J. Meng, F. S. Xiao, *J. Am. Chem. Soc.* 134, 15173 (2012). <https://doi.org/10.1021/ja3044954>
- [23] E. Ofer-Rozovsky, M. Arbel Haddad, G. Bar Nes, A. Katz, *J. Mater. Sci.* 51, 4795 (2016)  
<https://doi.org/10.1007/s10853-016-9767-0>
- [24] M. Fechtelkord, B. Posnatzki, J. C. Buhl, *Chem. Mater.* 13, 1967 (2001)  
<https://doi.org/10.1021/cm001136z>
- [25] R. Bian, J. Zhu, Y. Chen, Y. Yu, S. Zhu, L. Zhang, M. Huo, *RSC Adv.* 9, 36248 (2019)  
<https://doi.org/10.1039/C9RA06940B>